Appl Microbiol Biotechnol (2014) 98:2533–2543
DOI 10.1007/s00253-013-5123-3

Structural characteristics of thermostable immunogenic outer membrane protein from *Salmonella enterica* serovar Typhi

Gulam Rabbani · Jasmine Kaur · Ejaz Ahmad · Rizwan Hasan Khan · S. K. Jain

Received: 10 April 2013 / Revised: 14 June 2013 / Accepted: 10 July 2013 / Published online: 15 August 2013

Abstract In this work, we explored the acid-induced unfolding pathway of non-porin outer membrane protein (OMP), an immunogenic protein from *Salmonella* Typhi, by monitoring the conformational changes over a pH range of 1.0–7.0 by circular dichroism, intrinsic fluorescence, ANS binding, acrylamide quenching, and dynamic light scattering. The spectroscopic measurements showed that OMP in its native state at pH 7.0 exists in more stable and compact conformation. In contrast, at pH 2.0, OMP retains substantial amount of secondary structure, disrupted side chain interactions, increased hydrodynamic radii, and nearly four-fold increase in ANS fluorescence with respect to the native state, indicating that MG state exists at pH 2.0. Quenching of tryptophan fluorescence by acrylamide further confirmed the accumulation of a partially unfolded state between native and unfolded state. The effect of pH on the conformation and thermostability of OMP points towards its heat resistance at neutral pH (T_m~69 °C at pH 7.0, monitored by change in $MRE_{222\ nm}$). Acid unfolded state was also characterized by the lack of a cooperative thermal transition. All these results suggested that acid-induced unfolded state of OMP at pH 2.0 represented the molten globule state. The chemical denaturation studies with GuHCl and urea as denaturants showed dissimilar results. The chemical unfolding experiments showed that in both far-UV CD and fluorescence measurements, GuHCl is more efficient than urea. GuHCl is characterized by low C_m (~1 M), while urea is characterized by high C_m (~3 M). The fully unfolded states were reached at 2 M GuHCl and 4 M urea concentration, respectively. This study adds to several key considerations of importance in the development of therapeutic agents against typhoid fever for clinical purposes.

Keywords Acid denaturation · Outer membrane protein · Circular dichroism · Dynamic light scattering · Guanidine hydrochloride denaturation · Molten globule · *Salmonella enterica* serovar Typhi · Urea denaturation

Introduction

Salmonella enterica subspecies *enterica* serovars Typhi and Typhimurium are important human pathogens with distinctly different lifestyles (Barquist et al. 2013). *Salmonella* species cause typhoid fever and gastroenteritis in humans and pose a global threat to human health (Valdez et al. 2009). This potentially fatal systemic illness affects at least 21 million people annually, primarily in developing countries (Barquist et al. 2013; Bhutta and Threlfall 2009; Kothari et al. 2008). *Salmonella* also infects a broad array of animals, resulting in diseases ranging from gastroenteritis to life-threatening systemic infections (Chiu et al. 2004; McClelland et al. 2001). The outer membrane protein (OMP) from Gram-negative bacteria (*Salmonella* Typhi) is a major immunogenic target to synovial fluid lymphocytes of patients with reactive arthritis (ReA)/undifferentiated spondyloarthropathy (uSpA) (Pocanschi et al. 2013).

The OMPs of Gram-negative bacteria are synthesized in the cytoplasm and have to cross the inner membrane before being assembled into a correctly folded state in the outer membrane. Proteins are usually unfolded by chemical and physical treatments, which lead to alterations on their conformations (Dobson 2003; Fersht and Daggett 2002). One of the common methods of denaturing proteins is heating. Reports on conformational state of the denatured proteins have varied

Gulam Rabbani and Jasmine Kaur equally contributed to this paper.

Electronic supplementary material The online version of this article (doi:10.1007/s00253-013-5123-3) contains supplementary material, which is available to authorized users.

G. Rabbani · E. Ahmad · R. H. Khan (✉)
Interdisciplinary Biotechnology Unit, Aligarh Muslim University, Aligarh 202002, India
e-mail: rizwanhkhan@hotmail.com

J. Kaur · S. K. Jain
Department of Biotechnology, Faculty of Science, Hamdard University, New Delhi 110062, India

from apparently fully unfolded to substantial remaining structure (Goto et al. 1990). Unfolding caused by structural changes of proteins significantly influences their functional properties and results in pathological consequences in organisms (Lauren et al. 2009; Selkoe 2003; Tsigelny et al. 2008).

The structural stability and folding of OMP from *Salmonella* Typhi have been poorly understood at the present stage. OMP is involved in a wide range of physiological and disease processes. Here, in this article, we report folding/unfolding behavior of strategically important parasitic proteins and their structural consequence relevance, as well as the influence of the conformation of protein through the formation of molten globule state in acidic pH condition. We study the conformational stability of OMP in acidic pH interval to try to understand how the OMP can remain stable and functional at acidic pH values.

Materials and methods

Recombinant OMP was purified from Gram-negative *Salmonella* Typhi method described by Hamid and Jain (2008). Guanidine hydrochloride (GuHCl) urea and 1-anilino-8-napthalene sulfonate (ANS) were purchased from Sigma Chemical Co. All other reagents used in the study were of analytical grade.

pH-induced unfolding of OMP were carried out in 20 mM of KCl–HCl (pH 0.8–1.6), Gly-HCl (pH 1.8–3.0), Na-acetate (pH 3.5–5.0), and Na-phosphate (pH 6.0–7.0) buffers. All the buffers were passed through 0.45-μm filter. Protein samples were incubated for 12 h at room temperature in different pH before spectroscopic measurements were recorded.

Protein concentration determination

Stock of OMP prepared in 20-mM sodium phosphate buffer, pH 7.0, and protein concentration determined from the value of molar extinction coefficient 42,650 M^{-1} cm^{-1} at 280 nm. The molar extinction coefficient were obtained by entering the amino acid sequence in ExPASy-ProtParam tool (http://web.expasy.org/protparam) using 49 kDa molecular weight (Hamid and Jain 2008).

Circular dichroic measurements

CD measurements were carried out with a Jasco spectropolarimeter (J-815) equipped with a Jasco Peltier-type temperature controller (PTC-424S/15). The instrument was calibrated with D-10-camphorsulphonic acid. Spectra collected in a cell of 1 mm were 4 μM for far-UV CD with scan speed of 100 nm/min and response time of 1 s. Each spectrum was the average of two scans. The raw CD data obtained in millidegrees were converted to mean residue ellipticity (MRE) in degrees square centimeter per decimole, which is defined as

$$\mathrm{MRE} = \frac{\Theta_{\mathrm{obs}}(\mathrm{mdeg})}{10 \times n \times C \times l} \quad (1)$$

where Θ_{obs} is the CD in millidegrees, n is the number of amino acid residues, l is the path length of the cell, and C is the molar concentration. Helical content was calculated from the mean residue ellipticity (MRE) values at 222 nm using the following equation as described by Chen et al. (1972):

$$\%\alpha - \mathrm{helix} = \left(\frac{\mathrm{MRE}_{222\ \mathrm{nm}} - 2,340}{30,300}\right) \times 100 \quad (2)$$

The chemical denaturation experiment was done by equilibrating individual samples of OMP (4 μM) with various GuHCl and urea concentrations at pH 7.0 for 12 h at 25 °C.

The stock solution of 8 M GuHCl was prepared in 20-mM sodium phosphate buffer, pH 7.0, and change in pH was adjusted with KOH solution. Ten-molar urea solution was prepared in the above buffer (pH 7.0). The concentration of GuHCl and urea was determined using Mettler Toledo (Refracto 30PX). The ΔN value is the difference in refractive index between the GuHCl and urea solution and the buffer without GuHCl and urea. This ΔN value allows the determination of GuHCl and urea concentration according to the following equation (Pace 1986):

$$[\mathrm{GuHCl}] = 57.147(\Delta N) + 38.68(\Delta N)^2 - 91.60(\Delta N)^3 \quad (3)$$

$$[\mathrm{Urea}] = 117.66(\Delta N) + 29.753(\Delta N)^2 - 185.56(\Delta N)^3 \quad (4)$$

Data analysis of protein unfolding

Chemical and thermal denaturation data from CD and fluorescence spectroscopy were analyzed on the basis of two-state unfolding model. For a single-step unfolding process, N⇄U, where N is the native state and U is the unfolded state; the equilibrium constant, K_u, is

$$K_u = \frac{f_u}{f_n} \quad (5)$$

with f_u and f_n being the molar fraction of U and N, respectively.

$$f_d = \frac{(Y_{\mathrm{obs}} - Y_n)}{(Y_u - Y_n)} \quad (6)$$

where Y_{obs}, Y_n, and Y_u represent the observed property, the property of the native state, and the property of unfolded state, respectively.

The change in free energy of unfolding in water ΔG_u^o is obtained by the linear extrapolation model (Pace and Shaw 2000):

$$\Delta G_u = -RT\ln K_u \quad (7)$$

and

$$\Delta G = \Delta G_u^o - m(D) \quad (8)$$

where m is the experimental measure of the dependence of ΔG_u on denaturant, R is the gas constant (1.987 cal K^{-1} mol^{-1}), and T is the absolute temperature in Kelvin.

According to Eqs. 5–8, ΔG_u^o and m-values are obtained by nonlinear curve fitting to the transition curves. In the above fitting, the linear dependencies of f_u and f_n on denaturant (GuHCl, urea concentrations, and temperature) were also taken into consideration.

Tryptophanyl fluorescence measurements

Fluorescence measurements were performed on a Hitachi Spectrofluorometer (F-4500). The fluorescence spectra were measured at 25±0.1 °C with a 1 cm path length cell. The fluorescence was measured by exciting the protein at 280 nm, and emission spectra were recorded in the range of 300–400 nm. Both the excitation and emission slits were set at 10 nm. Protein concentration was kept at 4 μM.

ANS binding measurements

A stock solution of ANS was prepared in distilled water, and its concentration was determined using molar extinction coefficient of ε_M=5,000 M^{-1} cm^{-1} at 350 nm. For ANS binding experiments, the molar ratio of protein to ANS was 1:20. The excitation wavelength was set at 380 nm, and the emission spectra were taken in the range of 400–600 nm. Both the excitation and emission slits were set at 10 nm. Protein concentration was kept at 4 μM.

Acrylamide quenching experiments

In the quenching experiments, aliquots of 2 M quencher stock solution were added to protein solutions (4 μM) to achieve the desired range of quencher concentration (0.01–0.2 M). Excitation wavelength was set at 295 nm in order to excite tryptophan residues only, and the emission spectrum was recorded in the range of 300–400 nm. The decrease in fluorescence intensity was analyzed by using the Stern–Volmer equation:

$$\frac{F_o}{F} = 1 + K_{sv}[Q] \quad (9)$$

where F_o and F are the fluorescence intensities of the protein in the absence and presence of quenchers. K_{sv} is the quenching constant, which was determined from the slope of the Stern–Volmer plot at lower concentrations of quencher, whereas [Q] is the molar concentration of the quencher.

Dynamic light scattering (DLS) measurements

Dynamic light scattering (DLS) measurements were carried out at 830 nm by using DynaPro-TC-04 DLS equipment (Protein Solutions, Wyatt Technology, Santa Barbara, CA, USA).

Samples were filtered through a microfilter (Whatman International, Maidstone, UK) having an average pore size of 0.22 μm to remove any unwanted particles or aggregates. The filtered samples are directly transferred into a 12-μl black quartz cell, and protein concentration was 10 μM. For the detail of the methodology, refer to Rabbani et al. (2011).

Calorimetric measurements

Thermal denaturation experiments were conducted on a VP-DSC microcalorimeter (MicroCal, Northampton, MA, USA) at 20 mM pH 7.0 (Na-phosphate buffer) and pH 2.0 (Gly-HCl buffer). The DSC scans were run between 30 °C and 80 °C at a rate of 1.0 °C min^{-1}. The experiments were performed using 10 μM OMP. The heat capacity curves, midpoint temperature (T_m), calorimetric enthalpy (ΔH_{cal}), and van't Hoff enthalpy (ΔH_{vH}) were analyzed using Origin 7.0 software.

Results

Molecular modeling study

OMP from *Salmonella* Typhi is a monomer of about 49 kDa and 447-amino acid residues long. As there is not any high resolved full-length structure of OMP from *Salmonella* Typhi in the Protein Data Bank, the protein was modeled by Phyre2 (Kelley and Sternberg 2009) by using the sequence as given in Supplementary Figure S1. For such a large intact protein, part of the structure was generated based on the remote homology/fold recognition approach by taking the template of Dnad from *Bacillus subtilis* (2 V79), whereas the rest 366 residues were built by ab initio method. Predicted 3D models were verified by PROCHECK (Laskowski et al. 1993), and validation of stereo-chemical quality of the model was performed

through ERRAT, PDBSUM, and Verify3D. The structure was visualized by PyMol version 0.99 (DeLano 2002). Most proteins, however, possess multiple Trp residues, and the overall protein emission, naturally, yields only average information on the protein structure. OMP is a multitryptophan-containing protein (Trp88, 138, 176, 324, and 366). Trp88 is located at the central part of helix 1 region. Trp138 is located at the large N-terminal helix (Fig. 1). The even distributions of the five Trp in OMP make Trp fluorescence an excellent probe for monitoring the structural changes of the protein. Analysis of the accessible surface area of these Trp by the InterProSurf (Negi et al. 2007) indicates the following accessibility order: Trp176>Trp366>Trp38>Trp324>Trp88. Out of the total accessible surface area (29,413 $Å^2$) of the OMP, apolar residues contribute in greater extent (19,761 $Å^2$) than the polar residues (9,651 $Å^2$). Supplementary Figure S2 demonstrated the distribution of OMP amino acid residues. In Supplementary Figure S3, Ramachandran plot analysis showed that 67.5 % of all residues are located in the most favored regions, 22.6 % are in additionally allowed regions, 4.4 % residues fell in generously allowed regions, and 5.5 % are in disallowed regions (Table S1 Supplementary information).

Acid denaturation of OMP

Secondary structure conformational alterations monitored by far-UV CD measurements

The regular secondary structures (α-helix and β-sheets) are known to exhibit characteristic CD spectra in the far-UV (250–200 nm) range from which secondary structural content of the protein can be determined (Rabbani et al. 2011). The far-UV CD spectra of OMP were recorded over the pH range 1.0–7.0 to investigate the influence of pH on protein structure as shown in Fig. 2a. OMP at pH 7.0 exhibited the well characteristic spectra of α-helical proteins (minima at 222 and 208 nm) as shown in Fig. 2a. The secondary structural

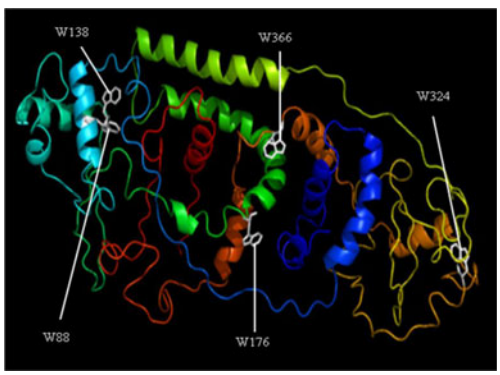

Fig. 1 Cartoon representation of OMP as drawn in PyMol. The polypeptide backbone composed by α-helices is shown by *coiled ribbons* and are connected by *loops*. The five Trp residues (W88, W138, W176, W324, and W366) are presented in *white stick*

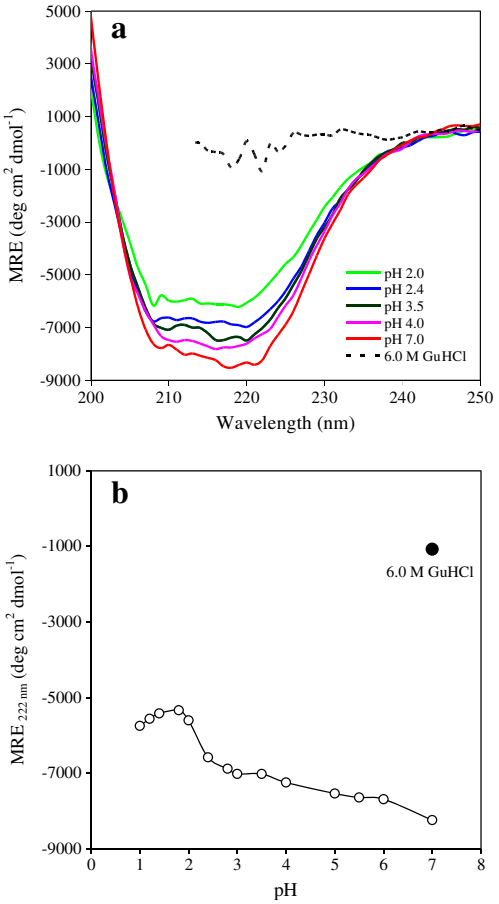

Fig. 2 **a** Far-UV CD spectra of OMP at pH 7.0, 4.0, 3.5, 2.4, and 2.0, and 6.0 M GuHCl denatured state, respectively. **b** Effect of pH on $MRE_{222\ nm}$ of OMP at different pH (*open circles*) and 6.0 M GuHCl (*closed circles*)

contents estimated from the Chen et al. method (Eq. 2) are tabulated in Table 1. Figure 2b shows the percent loss of α-helical structures for OMP as pH changes from 7.0 to 1.0. The average helical contents of OMP remained equal up to pH 5.0. At pH 7.0, the OMP shows higher helicity (35 %) as compared to the OMP at acidic pH. There is a steady decrease in helicity values for pH 6.0 (33 %), pH 5.0 (32 %), and pH 2.0 (26 %). This suggests that neutral pH has a greater secondary structural integrity and stability as compared to the acid ones. However, at very low pH 2.0, all the proteins got unfolded by losing their native secondary structure. Further, the $\theta_{208}/\theta_{222}$ ratio for the OMP appears nearly identical from pH 7.0 to 2.0, which is between 0.92 and 0.95 (Table 1). The ratio of $\theta_{208}/$

Table 1 Far-UV CD spectroscopic properties of OMP at different pH and under denatured condition

State	pH	$MRE_{208\ nm}$	$MRE_{222\ nm}$	α-helix (%)	$\theta_{208}/\theta_{222}$
Native	7.0	−7,617	−8,239	35	0.92
Molten globule	2.0	−6,169	−5,602	26	1.10
6.0 M GuHCl	7.0	–	−1,072	11	–

θ_{222} possibly depends on structural packing of proteins. It varies from 0.8 to 5.0 for the native proteins, while it ranges only from 1.1 to 1.4 for the molten globule (MG) state. The obtained values of $\theta_{208}/\theta_{222}$ ratio for pH 2.0 are within the reported range for various proteins (Vassilenko and Uversky 2002).

Tertiary structure conformational alterations monitored by tryptophan fluorescence measurements

Intrinsic protein fluorescence, using tryptophan (Trp) as a reporter, provides a sensitive measure of protein tertiary structure and is widely used in protein folding studies. The microenvironmental modifications of OMP aromatic residues due to denaturation by pH were studied by monitoring the changes in the fluorescence spectra as a function of pH. In proteins, Trp is highly sensitive to the polarity of its surrounding environment, and OMP is a muti-Trp-containing protein. The native protein showed an emission maximum at 340 nm suggesting the solvent exposure of some of the Trp residues is in the hydrophobic core of the protein at native condition (Fig. 3a). At pH 2.0, FI was reduced to 53 % along with a red shift of 10 nm indicating that Trp microenvironment became polar. Probably the structural perturbation (as observed in CD results) has fetched some of the Trp residues in a polar environment resulting in formation of a partially unfolded state at pH 2.0. Progressive lowering of pH led to rise in λ_{max} (wavelength maxima). The λ_{max} for 6.0 M GuHCl denatured state was red shifted to 355 nm with concomitant decrease in FI indicating that Trp residues are maximally exposed to the solvent. Figure 3b summarizes pH-dependent changes in FI and λ_{max} of OMP. A significant decline in FI and increase in λ_{max} was noticed between pH 7.0 and pH 2.0. As pH was lowered further from pH 2.0, the FI at 340 nm began to increase, crossing a value of 30 at pH 1.0 and finally reaching 32 at pH 1.0 with simultaneous increase in λ_{max}. These observations suggest that protein conformation under acidic conditions is different from native and 6.0 M GuHCl denatured state. This means that tryptophan fluorescence maxima are dependent on the hydrophobicity of the surrounding environment.

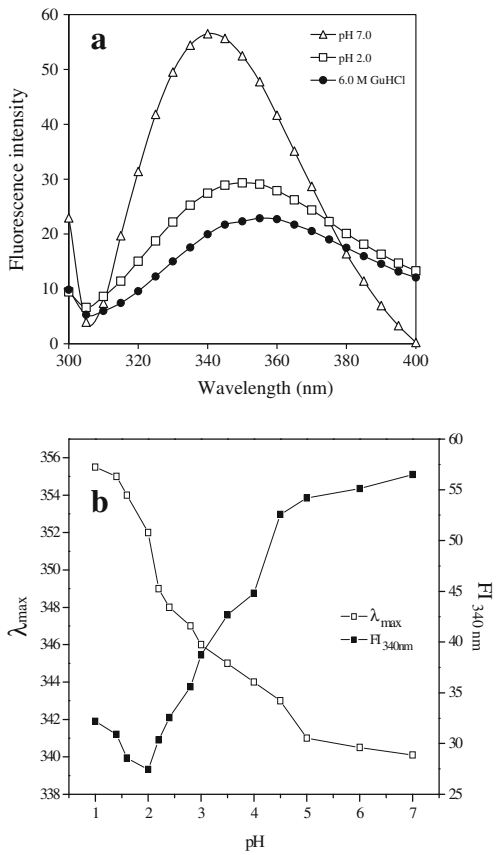

Fig. 3 **a** Intrinsic fluorescence spectra of OMP at pH 7.0 and 2.0, and 6.0 M GuHCl denatured, respectively. **b** Changes in intrinsic fluorescence at 340 nm (*closed squares*) vs. λ_{max} (*open squares*) of OMP at different pH

ANS binding experiments for interactions with exposed hydrophobic patches in OMP

ANS mainly binds to the structured and solvent accessible hydrophobic surface of proteins resulting in increase in fluorescence intensity with a substantial blue shift of the emission maxima. The folding and unfolding stages of the protein passing through various intermediates can thus be captured by ANS fluorescence experiments (Varshney et al. 2010). Here, we study the pH-induced structural changes in OMP by ANS fluorescence spectroscopy. The ANS emission maximum was recorded at 495 nm for native OMP at pH 7.0. This proves that native OMP has a compact structure with less hydrophobic surfaces exposed for ANS binding. However, at pH 2.0, the ANS emission maximum got shifted to 485 nm indicating greater solvent exposure of the hydrophobic patches of OMP as compared to native OMP (Fig. 4a). The fluorescence intensity of the ANS spectrum of OMP is at 480 nm as shown in Fig. 4b. This proves that during acid denaturation, some of the solvent-exposed hydrophobic patches of OMP become inaccessible. The ANS binding to OMP increases with a drop in pH values from 7.0 to 2.0, which reveals greater solvent exposure of hydrophobic patches. However, below pH 2.0, the effect gets suddenly reversed showing decreased fluorescence intensity. Thus, less hydrophobic regions of OMP are now being exposed to solvent. At pH 2.0, OMP possibly attains an intermediate state with the maximum fluorescence intensity and a large solvent-exposed hydrophobic region. At pH 7.0, there was less ANS binding as a consequence of the disordered or unfolded structure.

Acrylamide quenching studies for tryptophan accessibility

Acrylamide quenching of tryptophan fluorescence serves as a convenient method to probe tryptophan environments in proteins (Ahmad et al. 2012). Figure 5a shows a Stern–Volmer

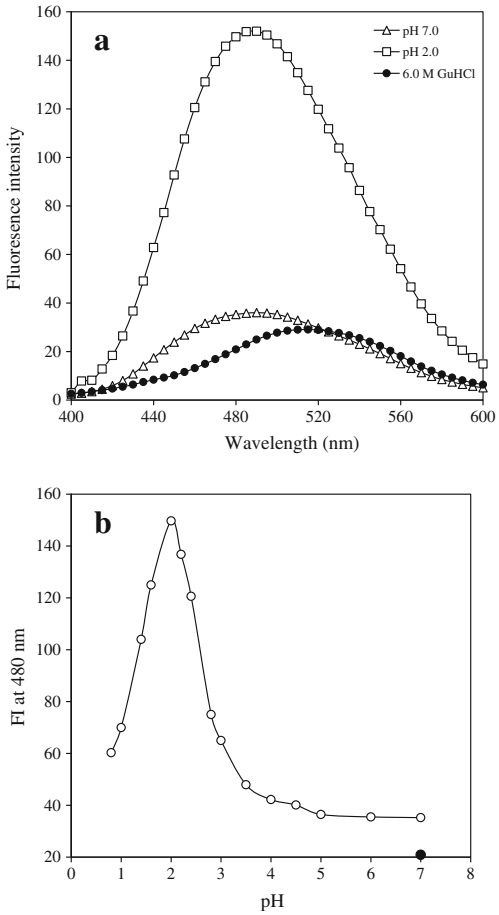

Fig. 4 ANS binding to OMP at pH 7.0 and 2.0, and 6.0 M GuHCl denatured, respectively. **b** Change in extrinsic fluorescence at 480 nm of OMP at different pH (*open squares*) and 6.0 M GuHCl (*closed squares*)

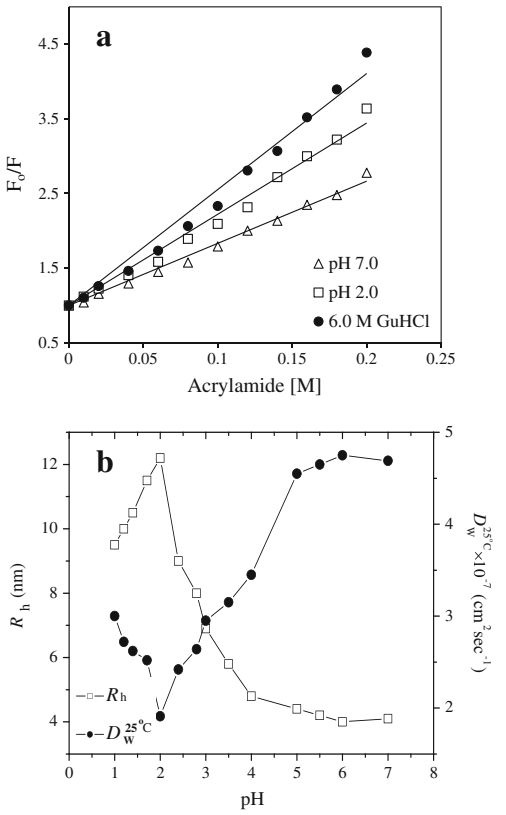

Fig. 5 **a** Stern–Volmer plots for acrylamide quenching of Trp fluorescence of OMP. **b** Trends of the translational diffusion coefficients ($D_W^{25°C}$) and the hydrodynamic radii (R_h) for OMP as a function of pH

plot of acrylamide quenching of tryptophans of native, molten globule (MG) state, and the unfolded protein in 6.0 M GuHCl. The slope (K_{sv}) of such plots is related to the degree of exposure (accessibility) of the tryptophans. Table 2 shows the quenching parameters obtained by analyzing the Stern–Volmer plots. The Stern–Volmer constant (K_{sv}) for the native OMP was found to be 8.3 M^{-1}. However, the value of K_{sv} for the molten globule state is 12 M^{-1}. The Stern–Volmer plot indicates that the aromatic amino acids at pH 2.0 are more exposed compared to the native folded conformation at pH 7.0; therefore, tryptophan fluorescence is quenched more in the case of the former. For the fully denatured protein in 6.0 M GuHCl, the K_{sv} value becomes quite large, being 16 M^{-1}, respectively, indicating a large increase in solvent exposure of tryptophan residues.

OMP self-association monitored by dynamic light scattering

Before DLS, measurements of OMP samples were incubated at 25 °C for 12 h to achieve the desired unfolded state under different pH condition and in 6.0 M GuHCl denatured states. It has been observed that R_h values of native OMP at pH 7.0 are 4.1 nm. The DLS results indicated a markedly reduced R_h, suggesting that the major component of OMP may consist of monomer. In contrast, OMP prepared in pH 2.0 exhibits a much larger size (12.2 nm) and a significantly higher percent polydispersity. The results indicated that the effect of pH may reflect some type of conformational changes upon lowering the pH favors self-association of OMP. Maximum R_h (23.8 nm) was observed for 6.0 M GuHCl denatured state

Table 2 Summary of the results of intrinsic and extrinsic fluorescence at different pH and under denatured condition analysis of OMP

State	pH	Intrinsic fluorescence		ANS binding		Acrylamide quenching
		FI_{340} (nm)	λ_{max} (nm)	FI_{480} (nm)	λ_{max} (nm)	K_{sv} (M^{-1})
Native	7.0	57	340	35	495	8.3
Molten globule	2.0	27	350	150	485	12
6.0 M GuHCl	7.0	20	355	21	520	16

Summary of parameters obtained from Stern–Volmer analysis (Eq. 9) of the solute quenching studies of OMP

indicating the existence of a remarkably unfolded and expanded conformation. A similar pattern was observed in apparent molecular weight for pH-induced unfolding of OMP (Table 3), while hydrodynamic radii and translational diffusion coefficient ($D_W^{25°C}$), which describes the property of molecules in solution phase, are inversely associated to each other. As a result, the values for $D_W^{25°C}$ followed the opposite pattern with respect to R_h (Fig. 5b). A low value of polydispersity (P_d~20 %) suggests the existence of an almost homogenous species and that protein behaved as monomer under all the conditions studied.

Thermostability monitored by circular dichroism spectroscopy and differential scanning calorimetry (DSC) measurements

Temperature-induced denaturation of the OMP secondary structures were monitored by following the loss of ellipticity at 222 nm using CD spectroscopy. The temperature at midpoint of temperature (T_m) was determined by fitting the temperature dependence of ellipticity into a two-state folding–unfolding reaction mechanism model. Most of the proteins are characterized by well-defined three-dimensional structures, which in general exist only within the limits of specific environmental conditions. Outside these conditions, proteins exhibit denatured and structurally unfolded states. Ellipticity plots, at 222 nm, are shown, as a function of temperature, together with the two-state model fits (Eq. 5). The thermal stability curve of OMP at pH 7.0 and pH 2.0 shows that the greatest thermal stability is observed near neutral pH. This result indicates cooperativity at pH 7.0 and absence of cooperativity as expected for a non-compact structure at pH 2.0. At pH 7.0, the secondary structure of OMP was found to be unperturbed up to 50 °C (Fig. 6a). At pH 7.0, the curve shows a single-phase transition having estimated T_m of 69 °C. OMP at pH 2.0 appears to be less stable than the native OMP with a melting temperature (T_m) of ~40 °C. These results suggest that ordered and more stable secondary occurs at neutral pH, while at pH 2.0, OMP becomes disordered and thermally less stable. Therefore, this considers that the classical acid-induced molten globule state of OMP exists at pH 2.0.

Table 3 pH dependence comparison of the hydrodynamic radii (R_h) and translational diffusion coefficients ($D_W^{25°C}$) from dynamic light scattering (DLS) experiments describing different states of OMP

State	pH	App. M.W. (kDa)	R_h (nm)	$D_W^{25°C} \times 10^{-7}$ ($cm^2 s^{-1}$)	P_d (%)
Native	7.0	51	4.1	4.69	18.3
Molten globule	2.0	79	12.2	1.91	17.3
6.0 M GuHCl	7.0	164	23.8	1.75	19.5

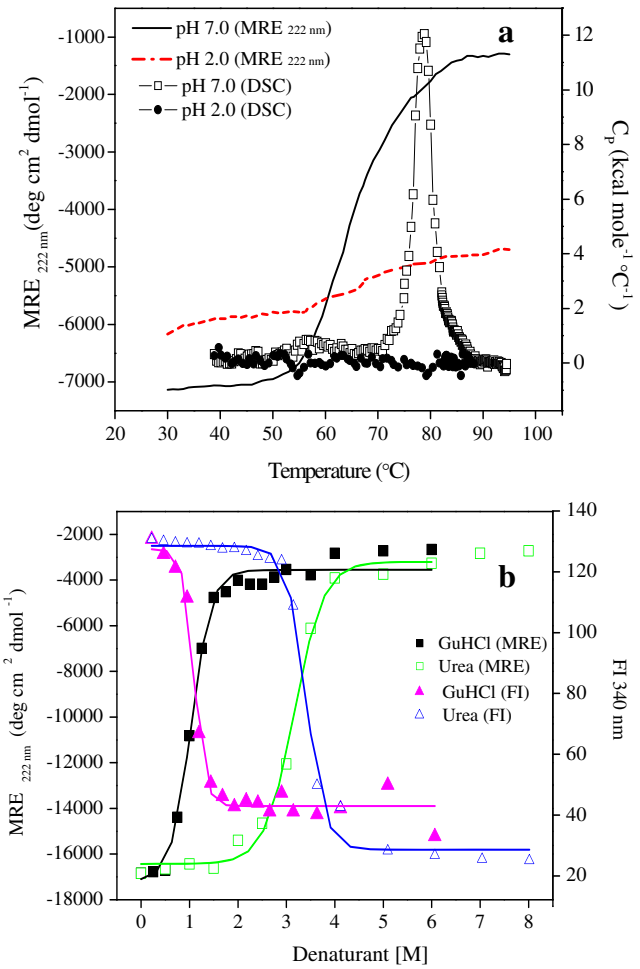

Fig. 6 **a** Temperature-induced denaturation profile showing changes in $MRE_{222\ nm}$ of OMP at pH 7.0 and pH 2.0. Calorimetric melting profile of OMP: at 10 μM, and at pH 7.0 and 2.0. **b** GuHCl and urea-induced unfolding of OMP at pH 7.0. Unfolding transition monitored by following the changes in $MRE_{222\ nm}$ and $FI_{340\ nm}$

To further investigate the process of thermal denaturation, DSC was applied to monitor the heat capacity change of OMP during the thermal unfolding process. OMP exhibits pre-transition and post-transition baseline change. Figure 6a shows that there is one peak with a maximum at 78 °C, from 30 °C to 90 °C in the heat capacity transition curve of 10 μM OMP at pH 7.0 in sodium phosphate buffer with a scan rate of 60 °C/h (Fig. 6a). A simulated curve using the van't Hoff equation based on a two-state transition fits this DSC curve well. The ΔH_{cal} estimated directly from the DSC curve is 50 kcal/mol, which is close to the van't Hoff enthalpy (ΔH_{vH}) (51 kcal/mol). As expected, the acid unfolded MG state (pH 2.0) shows no thermal transition observed by DSC; it may be because of the unordered tertiary structure of OMP as shown in Fig. 6a. Similar results were obtained by far-UV CD spectroscopy for secondary structure of OMP.

Effect of guanidinium hydrochloride (GuHCl) and urea

Equilibrium denaturation studies by far-UV CD measurements

The far-UV CD senses secondary structure of the protein and serves as a useful technique to probe the secondary structure characteristics of the species involved during protein unfolding/folding. The chemical stability of OMP was investigated using chaotropic agents such as urea and guanidinium hydrochloride (GuHCl)-induced unfolding (Andersen et al. 2012). Figure 6b shows the GuHCl and urea unfolding curves, monitored using far-UV CD spectroscopy, and can be fitted by a two-state model using Eq. 5. Inspection of the individual curves yields denaturant concentrations at the midpoint of the transitions, C_m, of 1.0 M for the GuHCl. The further addition of GuHCl up to 2.0 M led to the complete disruption of structure of native OMP (pH 7.0). Likewise, midpoint denaturant concentrations (C_m) of 3.1 M urea were found for OMP (Table 4). Further addition of GuHCl to 3.1 M led to the loss of structure (Fig. 6b) as the $MRE_{222\ nm}$ completely disappeared. OMP is quite stable in the presence of 1.5 M urea than the GuHCl 0.5 M since the $MRE_{222\ nm}$ signal of the OMP is essentially distinguishable and very different from that of unfolded protein under folded conditions. The chemical denaturant urea is highly cooperative in the change of secondary structure.

Equilibrium denaturation studies by tryptophan fluorescence measurements

Fluorescence spectra provide a sensitive means to characterize proteins and their conformations. The spectrum is determined mainly by the polarity of the environment of the tryptophan and tyrosine residues and by their specific interactions (Royer 2006). In this regard, the changes in both fluorescence wavelength and intensity were used to calculate the thermodynamic parameters of the unfolding process. The GuHCl-induced equilibrium unfolding transition of OMP was studied by intrinsic tryptophan fluorescence spectroscopy (Fig. 6b). Denaturation of OMP was monitored by measurement of intrinsic tryptophan fluorescence of the GuHCl-treated samples. The GuHCl and urea induced breakdown of the native tertiary structure ($FI_{340\ nm}$). The stability of the OMP suggests the significant differences between the dependencies of the free energy of unfolding upon denaturant. The corresponding values in the absence of denaturant (ΔG_u^o) were 2.5 and 6.2 kcal mol^{-1} for GuHCl and urea, respectively. The "*m* values" were very dissimilar at pH 7.0 for GuHCl and urea (2.7 and 1.9 kcal mol^{-1} M^{-1}), which suggests that almost the same states are involved in the unfolding transition. The C_m values under identical conditions were 0.95 and 3.2 M for GuHCl and urea, respectively, at pH 7.0 (Table 4). The differences in obtained results clearly show that GuHCl acts as a stronger denaturant than urea. This is a nontrivial observation since in general GuHCl is more efficient than urea in both dissociation and unfolding of proteins.

Table 4 Chemical unfolding parameters of OMP at pH 7.0

Parameter	GuHCl	Urea
$CD_{222\ nm}$	Cooperative	Cooperative
C_m (M)	1.0	3.1
ΔG_u^o(kcal mol^{-1})	4.0	3.5
m-value (kcal mol^{-1} M^{-1})	3.6	1.1
$FI_{340\ nm}$	Cooperative	Cooperative
C_m (M)	0.95	3.2
ΔG_u^o(kcal mol^{-1})	2.5	6.2
m-value (kcal mol^{-1} M^{-1})	2.7	1.9

Values of C_m, ΔG_u^o, and *m* values for GuHCl and urea induced unfolding of OMP are obtained from Eqs. 5–8

ΔG_u^o is change in unfolding free energy in the absence of denaturant

C_m is midpoint concentration

m-value is the denaturant dependence of the Gibbs free energy

Discussion

The structural characterization of OMP at different pH conditions is of great importance since this protein comes across varying pH conditions during its course of passage through the injectisome, at the interface of the host cell or within host cell environment (Yu et al. 2010). In the present work, we have attempted to reveal the conformational changes of OMP with gradual pH transitions, which can help us to better understand their mode of action in the infection process. Like other membrane pore-forming toxins, OMP also possibly undergoes structural reorientation at low pH ranges to attain competence for membrane penetration (Chenal et al. 2002; Faudry et al. 2006; Lindeberg et al. 2000).

The use of several biochemical and biophysical techniques has allowed us to study the conformational stability of OMP and the description of its unfolding pathway in the presence of different acidic pH values, chemical, and thermal denaturants. Exploring the structure and dynamics of intermediates of folding pathway is necessary not only to understand the mechanism of the protein folding but also to shed light on many natural or disease-related processes and biotechnological applications. Therefore, unfolding behavior and kinetics were studied for OMP as a model for bacterial protein. In the far-UV CD region, native OMP revealed two well-resolved negative peaks at 208 and 222 nm. The CD signals at 222 nm were more prominent, indicating high level of structural integrity of the protein. Significantly larger changes were observed in the CD spectra recorded at pH 2.0, suggesting the

occurrence of a pH-induced unfolding transition in this pH range. The OMP loses all of its secondary structural integrity around 2 M GuHCl or 4 M urea, as it is evident by complete disappearance of all the characteristic peaks in far-UV CD spectra measurements. In principle, unfolded states are rather heterogeneous, and the mechanisms leading to unfolded states are rather different for thermal, pH, or GuHCl and urea-induced unfolding (Ahmad et al. 2011).

Loss of tertiary structure of the protein was monitored by intrinsic tryptophan fluorescence spectroscopy. Solutions of OMP were excited at 295 nm; this shows fluorescence emission maximum (λ_{max}) at 340 nm in the native state, whereas it shifts to 355 nm with 60–65 % drop in intensity under complete chemical denatured conditions. Similar shifts in λ_{max} for various proteins under chemical-induced denaturation have been reported previously (Charalambous et al. 2009; Cremades et al. 2008; Devaraneni et al. 2012). Consequently, at pH 7.0, the tryptophan of OMP remains partially exposed to the solvent, as evident from the tryptophan emission spectrum. The OMP at pH 7.0 shows λ_{max} at 340 nm, indicating greater solvent exposure of the tryptophan residues. The fluorescence spectroscopic results also suggest that OMP acts differently with changing pH conditions both as individual protein and in the complex form with ANS. The existence of OMP as a molten globule is confirmed by large exposed hydrophobic patches on the protein from our ANS binding studies.

Environmental stresses such as those used in this study are physiologically relevant. Significant urea concentrations are known to accumulate in cells and in the mammalian renal medulla (kidney), reaching levels that alter functional and structural properties of intracellular proteins (Elam et al. 2013). The two denaturants act differently since GuHCl is a salt while urea is a neutral molecule. For example, more compact structures of the acid unfolded states as compared to chemical unfolded states would also explain more exposed tryptophan residues which exhibit greater red shifts. OMP demonstrates environment-dependent variation in unfolding pathways (Fig. 6b). Chemical-induced denaturation leads to complete unfolding of the protein. Furthermore, the conformational scrambling of both unfolded states might be different due to different mechanisms of denaturing the proteins. It is obvious that this also may have different effects on the microenvironment of tryptophan residues. Such general observations were also found to be true for the unfolding process of OMP.

Molecular size characterized by DLS measurement proves the low pH-induced unfolding leads to the monomeric association with an intermediate state, due to structural relaxation in protein molecule. This is related to the fact that DLS technique detects global changes of the protein molecule. Our DLS data show that the lowering of pH values in the order pH 7.0>pH 6.0>pH 5.0>pH 4.0>pH 3.0>pH 2.0 favors the unfolding process led by an increase in hydrodynamic radii. Our present results are consistent with previous observations, based on DLS, enhanced ANS binding, retention of significant secondary structures, and disrupted tertiary structure. All these results suggested that the acid-induced state of OMP at pH 2.0 is characterized as molten globule state.

The thermal investigation is previously not reported for OMP, so this study opens up a new dimension for research with the possibility of obtaining new insight in similar classes of proteins. This probably allows the protein to fold and function in even challenging environment that may differ from its normal environment under certain circumstances. Such ability might have also helped proteins to survive evolutionary selection pressure and even to attain environment-specific conformations since we now know that most proteins acquire closely similar conformations instead of a unique conformation.

To further explore if the thermal unfolding reaction was reversible or not, the sample was heated at a constant heating rate. After the thermal denaturation transitions went to completion, the OMP solutions were cooled down to 20 °C at the same scan speed, and further, the OMP samples are heated up to 90 °C. From the obtained results, it is clear that the secondary structures of the native polypeptide were not recovered after the sample was cooled down to the initial temperature by $MRE_{222\ nm}$ measurements. Similarly, no detectable recovery in the secondary structures was observed for other heating rates (data not shown). These results indicate that thermal unfolding of OMP is highly irreversible. The irreversible process seems to be the more common case for most proteins, such as peroxidase (Zamorano et al. 2009), triose phosphate isomerase (Shi et al. 2008), α-amylase (Sugahara et al. 2013), yeast hexokinase B (Ramshini et al. 2008), and latex amine oxidase (Amani et al. 2007).

Salmonella Typhi is a pathogenic bacterium that causes a number of infectious diseases such as gastroenteritis and typhoid fever (Kaur and Jain 2012). Before orally ingested enteric pathogens *Salmonella* can reach their target host cells, they must first survive their encounter with the low pH of the human stomach, approximately pH 2.0 following a fast. The low pH of the gastric environment provides *Salmonella* Typhi the ability to survive at low pH. This is an extremely hostile environment, thus *Salmonella* contains multiple inducible systems to aid in survival at low pH (Brenneman et al. 2013; Kaur and Jain 2012). Enteric pathogens, in order to gain entrance into the intestine and cause disease, must survive the acid pH of the stomach. Pathogenic species that prefer to grow at neutral pH exhibit widely varying abilities to survive pH extremes. However, there is increasing evidence that molten globules are common and that they play a key role in a wide variety of physiological processes, including translocation across membranes, increased affinity for membranes, binding to liposome and phospholipids, protein trafficking, extracellular secretion, and the control and regulation of the

cell cycle (Morrow et al. 2002). Structural stability can also be seen in Diphtheria toxin T and SARS-CoV main protease, while other proteins, such as human alkaline phosphatase, human apolipoprotein E, and malic enzyme, have been shown to undergo a significant molten globule transition state during the unfolding process (Chang et al. 2007; Hung and Chang 2001; Morrow et al. 2002; Rodnin et al. 2008). In addition, the development of methods to fold integral membrane proteins to their active form is of significant technological importance.

Acknowledgments G. Rabbani and J. Kaur acknowledge the Council of Scientific and Industrial Research (CSIR), New Delhi, India and Indian Council of Medical Research (ICMR), New Delhi, India, respectively, for financial assistance in the form of Senior Research Fellowship (SRF).

References

Ahmad E, Sen P, Khan RH (2011) Structural stability as a probe for molecular evolution of homologous albumins studied by spectroscopy and bioinformatics. Cell Biochem Biophys 61:313–325

Ahmad E, Rabbani G, Zaidi N, Ahmad B, Khan RH (2012) Pollutant-induced modulation in conformation and beta-lactamase activity of human serum albumin. PLoS One 7:e38372

Amani M, Moosavi-Movahedi AA, Floris G, Mura A, Kurganov BI, Ahmad F, Saboury AA (2007) Two-state irreversible thermal denaturation of *Euphorbia characias* latex amine oxidase. Biophys Chem 125:254–259

Andersen KK, Wang H, Otzen DE (2012) A kinetic analysis of the folding and unfolding of OmpA in urea and guanidinium chloride: single and parallel pathways. Biochemistry 51:8371–8383

Barquist L, Langridge GC, Turner DJ, Phan MD, Turner AK, Bateman A, Parkhill J, Wain J, Gardner PP (2013) A comparison of dense transposon insertion libraries in the *Salmonella* serovars Typhi and Typhimurium. Nucleic Acids Res 41:4549–4564

Bhutta ZA, Threlfall J (2009) Addressing the global disease burden of typhoid fever. JAMA 302:898–899

Brenneman KE, Willingham C, Kong W, Curtiss R, 3rd, Roland KL (2013) Low pH rescue of acid-sensitive *Salmonella* Typhi strains by a rhamnose-regulated arginine decarboxylase system. J Bacteriol 195:3062–3072

Chang HP, Chou CY, Chang GG (2007) Reversible unfolding of the severe acute respiratory syndrome coronavirus main protease in guanidinium chloride. Biophys J 92:1374–1383

Charalambous K, O'Reilly AO, Bullough PA, Wallace BA (2009) Thermal and chemical unfolding and refolding of eukaryotic sodium channel. Biochim Biophys Acta 1788:1279–1286

Chen YH, Yang JT, Martinez HM (1972) Determination of the secondary structures of proteins by circular dichroism and optical rotatory dispersion. Biochemistry 11:4120–4131

Chenal A, Savarin P, Nizard P, Guillain F, Gillet D, Forge V (2002) Membrane protein insertion regulated by bringing electrostatic and hydrophobic interactions into play. A case study with the translocation domain of diphtheria toxin. J Biol Chem 277:43425–43432

Chiu CH, Su LH, Chu C (2004) *Salmonella enterica* serotype Choleraesuis: epidemiology, pathogenesis, clinical disease, and treatment. Clin Microbiol Rev 17:311–322

Cremades N, Bueno M, Neira JL, Velazquez-Campoy A, Sancho J (2008) Conformational stability of *Helicobacter pylori* flavodoxin: fit to function at pH 5. J Biol Chem 283:2883–2895

DeLano WL (2002) The PyMOL molecular graphics system. DeLano Scientific, San Carlos

Devaraneni PK, Mishra N, Bhat R (2012) Polyol osmolytes stabilize native-like cooperative intermediate state of yeast hexokinase A at low pH. Biochimie 94:947–952

Dobson CM (2003) Protein folding and misfolding. Nature 426:884–890

Elam WA, Schrank TP, Campagnolo AJ, Hilser VJ (2013) Temperature and urea have opposing impacts on polyproline II conformational bias. Biochemistry 52:949–958

Faudry E, Vernier G, Neumann E, Forge V, Attree I (2006) Synergistic pore formation by type III toxin translocators of *Pseudomonas aeruginosa*. Biochemistry 45:8117–8123

Fersht AR, Daggett V (2002) Protein folding and unfolding at atomic resolution. Cell 108:573–582

Goto Y, Takahashi N, Fink AL (1990) Mechanism of acid-induced folding of proteins. Biochemistry 29:3480–3488

Hamid N, Jain SK (2008) Characterization of an outer membrane protein of *Salmonella enterica* serovar Typhimurium that confers protection against typhoid. Clin Vaccine Immunol 15:1461–1471

Hung HC, Chang GG (2001) Multiple unfolding intermediates of human placental alkaline phosphatase in equilibrium urea denaturation. Biophys J 81:3456–3471

Kaur J, Jain SK (2012) Role of antigens and virulence factors of *Salmonella enterica* serovar Typhi in its pathogenesis. Microbiol Res 167:199–210

Kelley LA, Sternberg MJ (2009) Protein structure prediction on the Web: a case study using the Phyre server. Nat Protoc 4:363–371

Kothari A, Pruthi A, Chugh TD (2008) The burden of enteric fever. J Infect Dev Ctries 2:253–259

Laskowski RA, MacArthur MW, Moss DS, Thornton JM (1993) PROCHECK: a program to check the stereochemical quality of protein structures. J Appl Crystallogr 26:283–291

Lauren J, Gimbel DA, Nygaard HB, Gilbert JW, Strittmatter SM (2009) Cellular prion protein mediates impairment of synaptic plasticity by amyloid-beta oligomers. Nature 457:1128–1132

Lindeberg M, Zakharov SD, Cramer WA (2000) Unfolding pathway of the colicin E1 channel protein on a membrane surface. J Mol Biol 295:679–692

McClelland M, Sanderson KE, Spieth J, Clifton SW, Latreille P, Courtney L, Porwollik S, Ali J, Dante M, Du F, Hou S, Layman D, Leonard S, Nguyen C, Scott K, Holmes A, Grewal N, Mulvaney E, Ryan E, Sun H, Florea L, Miller W, Stoneking T, Nhan M, Waterston R, Wilson RK (2001) Complete genome sequence of *Salmonella enterica* serovar Typhimurium LT2. Nature 413:852–856

Morrow JA, Hatters DM, Lu B, Hochtl P, Oberg KA, Rupp B, Weisgraber KH (2002) Apolipoprotein E4 forms a molten globule. A potential basis for its association with disease. J Biol Chem 277:50380–50385

Negi SS, Schein CH, Oezguen N, Power TD, Braun W (2007) InterProSurf: a web server for predicting interacting sites on protein surfaces. Bioinformatics 23:3397–3399

Pace CN (1986) Determination and analysis of urea and guanidine hydrochloride denaturation curves. Methods Enzymol 131:266–280

Pace CN, Shaw KL (2000) Linear extrapolation method of analyzing solvent denaturation curves. Proteins Suppl 4:1–7

Pocanschi CL, Popot JL, Kleinschmidt JH (2013) Folding and stability of outer membrane protein A (OmpA) from *Escherichia coli* in an amphipathic polymer, amphipol A8-35. Eur Biophys J 42:103–118

Rabbani G, Ahmad E, Zaidi N, Khan RH (2011) pH-dependent conformational transitions in conalbumin (ovotransferrin), a metalloproteinase from hen egg white. Cell Biochem Biophys 61:551–560

Ramshini H, Rezaei-Ghaleh N, Ebrahim-Habibi A, Saboury AA, Nemat-Gorgani M (2008) Thermally induced changes in the structure and activity of yeast hexokinase B. Biophys Chem 137:88–94

Rodnin MV, Posokhov YO, Contino-Pepin C, Brettmann J, Kyrychenko A, Palchevskyy SS, Pucci B, Ladokhin AS (2008) Interactions of fluorinated surfactants with diphtheria toxin T-

domain: testing new media for studies of membrane proteins. Biophys J 94:4348–4357

Royer CA (2006) Probing protein folding and conformational transitions with fluorescence. Chem Rev 106:1769–1784

Selkoe DJ (2003) Folding proteins in fatal ways. Nature 426:900–904

Shi Y, Liu JH, Zhang HJ, Ding Y (2008) Equilibrium unfolding mechanism of chicken muscle triose phosphate isomerase. Protein Pept Lett 15:365–370

Sugahara M, Takehira M, Yutani K (2013) Effect of heavy atoms on the thermal stability of alpha-amylase from *Aspergillus oryzae*. PLoS One 8:e57432

Tsigelny IF, Crews L, Desplats P, Shaked GM, Sharikov Y, Mizuno H, Spencer B, Rockenstein E, Trejo M, Platoshyn O, Yuan JX, Masliah E (2008) Mechanisms of hybrid oligomer formation in the pathogenesis of combined Alzheimer's and Parkinson's diseases. PLoS One 3:e3135

Valdez Y, Ferreira RB, Finlay BB (2009) Molecular mechanisms of *Salmonella* virulence and host resistance. Curr Top Microbiol Immunol 337:93–127

Varshney A, Ahmad B, Rabbani G, Kumar V, Yadav S, Khan RH (2010) Acid-induced unfolding of didecameric keyhole limpet hemocyanin: detection and characterizations of decameric and tetrameric intermediate states. Amino Acids 39:899–910

Vassilenko KS, Uversky VN (2002) Native-like secondary structure of molten globules. Biochim Biophys Acta 1594(1):168–177

Yu XJ, McGourty K, Liu M, Unsworth KE, Holden DW (2010) pH sensing by intracellular *Salmonella* induces effector translocation. Science 328:1040–1043

Zamorano LS, Vilarmau SB, Arellano JB, Zhadan GG, Cuadrado NH, Bursakov SA, Roig MG, Shnyrov VL (2009) Thermal stability of peroxidase from *Chamaerops excelsa* palm tree at pH 3. Int J Biol Macromol 44:326–332